Fluorescence turn-on sensors for HSO_4^-†

Hyun Jung Kim,[a] Sankarprasad Bhuniya,[a] Rakesh Kumar Mahajan,*[b] Rajiv Puri,[b] Hongguang Liu,[c] Kyoung Chul Ko,[c] Jin Yong Lee*[c] and Jong Seung Kim*[a]

Received (in Cambridge, UK) 7th September 2009, Accepted 1st October 2009
First published as an Advance Article on the web 16th October 2009
DOI: 10.1039/b918324h

A coumarin-based derivative (1), a highly selective and sensitive turn-on fluorogenic probe for the detection of HSO_4^- ions in aqueous solution, has been designed and synthesized. Various spectroscopic and DFT calculations revealed that H-bonding between the phenolic –OH and imine nitrogen of 1 played a crucial role in its high selectivity for HSO_4^-.

Chemosensors based on ion-induced fluorescence changes are predominantly attractive because of the simplicity and low detection limit of fluorescence detection methods.[1–3] In the midst of it all, fluorescence 'turn-on' sensors for detection of anions of biological importance still remain a challenging aspect given that general anions can act as fluorescence quenchers.[4,5] Hence, much attention has been paid to the design of 'turn-on' anionic fluorescence sensors. Among the anions, hydrogen sulfate (HSO_4^-) is of particular interest owing to its established role in biological and industrial areas.[6] This amphiphilic anion eventually dissociates at high pH to generate toxic sulfate ion (SO_4^{2-}),[7] causing irritation of the skin and eyes and even respiratory paralysis. For these reasons, an improved method for the detection and sensing of HSO_4^- ions with high selectivity is of current interest in the chemosensor research field. Only a few examples of fluorogenic chemosensors showing absorbance or fluorescence changes upon HSO_4^- complexation have been reported;[8] however, selectivity remains questionable.

We herein report a new coumarin-based fluorescent sensor (**1**)[9] in Fig. 1 that exhibits a unique fluorescence change in the presence of the HSO_4^- ion and with high selectivity over other anions. To establish the mechanism of the fluorescence changes upon addition of HSO_4^-, two more analogues (**2** and **3**) were also prepared and their fluorescent properties examined.[9]

Compound **1** shows a characteristic UV-Vis absorbance band centered at 355 nm in 50% aqueous CH_3CN. In the presence of the HSO_4^- ion, the absorption band at 355 nm shifted to 370 nm

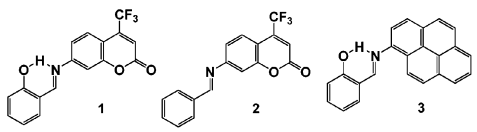

Fig. 1 Structures of fluorescent sensors **1–3**.

[a] *Department of Chemistry, Korea University, Seoul 136-701, Republic of Korea. E-mail: jongskim@korea.ac.kr; Fax: +82-2-3290-3121; Tel: +82-2-3290-3143*
[b] *Department of Chemistry, Guru Nanak Dev University, Amritsar 143005, India. E-mail: rakesh_chem@yahoo.com; Fax: +91-183-2258820*
[c] *Department of Chemistry, Sungkyunkwan University, Suwon 440-746, Republic of Korea. E-mail: jinylee@skku.edu*

† Electronic supplementary information (ESI) available: Experimental details. CCDC 746885. For ESI and crystallographic data in CIF or other electronic format see DOI: 10.1039/b918324h

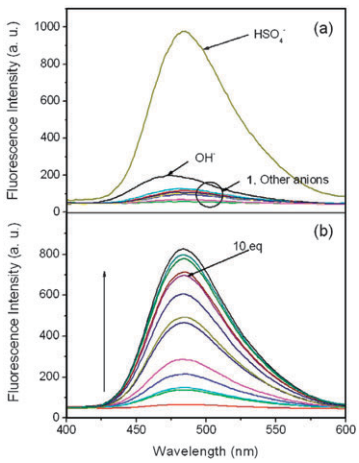

Fig. 2 (a) Fluorescence spectra of **1** (3.0 μM) λ_{ex} = 355 nm upon addition of TBA^+ salts of F^-, Cl^-, Br^-, I^-, $CH_3CO_2^-$, HSO_4^-, $H_2PO_4^-$, NO_3^-, and OH^- (50 equiv.) in 1 : 1 CH_3CN–H_2O (v/v). (b) Fluorescence titration spectra of **1** (3.0 μM) in 1 : 1 CH_3CN–H_2O (v/v) upon addition of TBA^+ HSO_4^- (0, 0.1, 0.3, 0.5, 1, 3, 5, 6, 7, 8, 10, 20, 30, 50, 100 equiv.) with excitation at 355 nm.

(Fig. S1,† S hereafter denotes Supporting Information). More interestingly, we observed a remarkable fluorescence increment of **1** at 485 nm upon addition of HSO_4^- to a solution of CH_3CN–H_2O (1 : 1) (Fig. 2a), whereas no meaningful fluorescence changes were noticed with other anions. The titration spectra of **1** with the HSO_4^- ion at 485 nm show a 13-fold fluorescence enhancement (Fig. 2b). Job's plot analysis of the fluorescence titration spectra exhibited a maximum at a 0.5 mol fraction of HSO_4^-, indicating formation of a 1 : 1 complex between **1** and the HSO_4^- ion (Fig. S2†). On the basis of both the 1 : 1 stoichiometry and fluorescence titration data from Fig. 2, the association constant of **1** for HSO_4^- was calculated to be 4.86×10^4 M^{-1}.[10]

The competitive binding aptitude of **1** with HSO_4^- over other anions was studied as shown in Fig. 3. The fluorescence intensity of **1** was quenched upon addition of various anion mixtures, including TBA^+ salts of: F^-; Cl^-; Br^-; I^-; $CH_3CO_2^-$; $H_2PO_4^-$; NO_3^-; OH^-. Upon gradual addition of HSO_4^- to the anion mixture, the fluorescence of **1** was revived, suggesting that **1** possesses an excellent selectivity for HSO_4^- over competitive anions.

Furthermore, the fluorescence changes of **1** (3.0 μM) in the absence and presence of 30 equiv. of HSO_4^-, in different pH environments, were studied and are described in Fig. S3.† Compound **1** gave an insignificant response to fluorescence changes under different pH conditions. However, upon addition of the HSO_4^- ion, we found a distinct increase in the emission

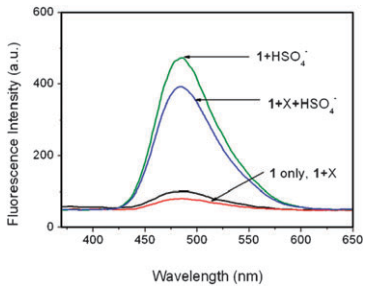

Fig. 3 Fluorescence spectra of **1** (3.0 μM) in 1 : 1 CH_3CN–H_2O (v/v) in the presence of HSO_4^- (50 equiv.) and TBA^+ salts of various anions (F^-, Cl^-, Br^-, I^-, CH_3COO^-, $H_2PO_4^-$, NO_3^-, OH^-, 50 equiv., respectively) with excitation at 355 nm.

bands of **1** at 485 nm between pH 4 and 10. Such broad pH spans in an aqueous milieu make it very useful in several applications, such as HSO_4^- detection in wastewater, industrial trade analysis, and physiological treatment.

To obtain insight into the binding mode of **1** with HSO_4^-, ^{1}H-NMR titration experiments were carried out (Fig. S4†). We found that the phenolic proton (Ha) had intramolecular H-bonding with the imine nitrogen at 12.6 ppm, which was conclusively evidenced by the X-ray crystal structure (Fig. S5†).‡ However, in the presence of HSO_4^-, the corresponding –OH peak disappeared, delineating that the intramolecular H-bonding of **1** is interrupted by coordination of HSO_4^- with **1**.

To examine the role of intermolecular H-bonding between the phenolic –OH and imine moiety and the role of the coumarin unit in the fluorescence changes of **1**, **2** was prepared without the hydroxy group and **3** with a pyrenyl moiety instead of coumarin. Upon addition of HSO_4^- to **2** and **3**, the observed fluorescence change of **2** was marginal and non-selective toward the anions, implying that the H-bonding between the phenolic –OH and the imine N in **1** plays a crucial role in the high selectivity of **1** for HSO_4^- ion over other anions (Fig. S6†). Similarly, compound **3** alone showed weak fluorescence (Fig. S7†); however, it increased in the presence of HSO_4^-, as noted for **1**. This observation suggests that 6-membered intramolecular H-bonding of phenolic –OH with the imine N initially contributed to the fluorescence quenching of **1**, which was then followed by selective blocking of the H-bonding by the HSO_4^- ion to give fluorescence enhancement of **1** and **3**.

To clarify the 'Off–On' fluorescence mechanism, density functional theory (DFT) calculations were performed with the B3LYP exchange functional employing 6-31G* basis sets using a suite of Gaussian 03 programs.[11] Fig. 4 shows the optimized structures of **1** and its complex with HSO_4^- (**1**-HSO_4^-). Compound **1** has an intramolecular hydrogen bond, whereas the **1**-HSO_4^- complex has three intermolecular H-bonds, one between the oxygen of the HSO_4^- and the hydrogen (–OH) of **1**, another between the hydrogen of the HSO_4^- and the oxygen (–OH) of **1**, and a third between the hydrogen of the HSO_4^- and the nitrogen of **1**. Thus, apparently **1** can interact strongly with the HSO_4^- ion.

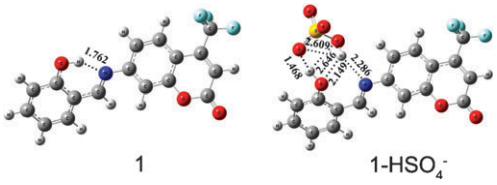

Fig. 4 Optimized structures of compound **1** and **1**-HSO_4^- and distances of the hydrogen bonds (Å).

Natural bond orbital (NBO) analyses (Fig. S8†) show a notable change in the charge of the N atom when **1** forms a complex with HSO_4^-. The charge of the N atom of **1**, **2**, and **1**-HSO_4^- is −0.527, −0.446, and −0.456, respectively. From these data, we noticed that the N atom of **1** possessed greater electron density even though it was exhibiting intramolecular H-bonding with the phenolic –OH group. In similar H-bonding systems, the electrons usually transfer from the nitrogen to the hydrogen, and as a consequence, the charge density on the N is reduced. This unusual negative charge allocation on the N of **1** leads to fluorescence quenching; nevertheless, it showed affinity to form a complex with HSO_4^- *via* an H-bond and consequently enhanced the fluorescence.

The 'Off–On' fluorescence mechanism of **1** is also explained by the widely accepted photo-induced electron transfer (PET) (Fig. S9†) mechanism.[12] Table 1 lists the dominant electron transitions with the two strongest absorptions, considering oscillator strength.

The nonbonding lone pair electrons of the nitrogen correspond to the HOMO in **1**, HOMO-1 in **2**, and HOMO-2 in **1**-HSO_4^-, while the occupied π-bonding (Fig. S10†) orbital characters of C=N are HOMO-1 in **1**, HOMO in **2**, and HOMO-4 in **1**-HSO_4^-, respectively. Since these π-bonding orbitals and the nitrogen lone pair orbitals possess small energy differences, the electronic transition from the nitrogen lone pair to the occupied π-bonding orbital was assumed to trigger the PET process, and thus lead to fluorescence quenching.

In Table 1, the oscillator strengths for the transitions from the nitrogen lone pair to the π* orbitals ($n \rightarrow \pi^*$) are 0.4084, 0.0346, and 0.2812 for **1**, **2**, and **1**-HSO_4^-, respectively, corresponding to the transition energies of 386, 314, and 443 nm, respectively. As mentioned above, these contributions cause the fluorescence quenching of **1**. The other important transitions take place at 341, 357, and 362 nm with oscillator strengths of 0.3488, 0.6360, and 0.2807 for **1**, **2**, and **1**-HSO_4^-, respectively. Thus, when a 355 nm light source is used for excitation, both transitions can take place for **1** and **2**. However, for **1**-HSO_4^-, the $n \rightarrow \pi^*$ transition may be very limited due to the transition energy (443 nm) being more deviated to 355 nm. For **2**, a very weak oscillator strength for the $n \rightarrow \pi^*$ transition also restricts the $n \rightarrow \pi^*$ transition. Thus, the fluorescence is 'turned-off' in **1**, while 'turned-on' for **2** and **1**-HSO_4^-.

The selective binding affinity toward HSO_4^- of **1** encouraged construction of an HSO_4^- ion-selective electrode PVC membrane

Table 1 Calculated TDDFT excitation properties containing the first and second highest oscillator strength of **1**, **2** and **1**-HSO_4^- in low excitation energy (λ > 310 nm)

Compound	Excitation	Excitation wavelength (nm)	Oscillator strength (au)
1	HOMO → LUMO	386	0.4084
	HOMO-1 → LUMO	341	0.3488
2	HOMO → LUMO	357	0.6360
	HOMO-1 → LUMO	314	0.0346
1-HSO_4^-	HOMO-2 → LUMO	443	0.2812
	HOMO-4 → LUMO	362	0.2807

Table 2 Composition and potential response characteristics of the HSO_4^- ion-selective electrode

PVC (mg)	DOS[a] (mg)	ToMA Cl[a] (mg)	Ionophore **1** (mg)	Linear range (M)	Detection limit (M)	Slope (mV/decade)
100.7	200.1	1.2	5.3	1.0×10^{-1} -1.0×10^{-5}	3.75×10^{-6}	−57.47

[a] DOS: Dioctyl sebacate as plasticizer; ToMA Cl: Tri-octyl methyl ammonium chloride.

based on **1** for the application. A sensor membrane incorporating **1** was prepared and assembled as previously reported.[13] The potentiometric cell used was Ag/AgCl (3.0 M KCl)/1.0×10^{-2} M $TBA^+HSO_4^-$/PVC membrane/Test solution/(3.0 M KCl) AgCl/Ag. The composition of this membrane is listed in Table 2.

In preliminary experiments, the ionophore **1** acted as an efficient ion carrier for the HSO_4^- anion in comparison to other examined anions (Fig. S11†). Most interestingly, the response time for sensing the HSO_4^- was less than 10 s (Fig. S12†) with a suitable operational pH for the sensor from 1.4 to 4.9 (Fig. S13†).

Next, the potentiometric selectivity coefficients over interfering ions were determined using the fixed interference method. Accordingly, potentiometric selectivity coefficients ($\log K^{Pot}_{HSO_4^-,B}$) can be evaluated by carrying out potential measurements on solutions containing fixed concentrations of interfering ions (1.0×10^{-2} M) and varying concentrations of the HSO_4^- anion. Table 3 shows the potentiometric selectivity coefficient data of the ionophore **1**–PVC membrane electrodes for interfering anions relative to the HSO_4^- ions. The selectivity coefficient pattern clearly indicates that the electrodes are selective for HSO_4^- over a number of other anions. The selectivity coefficient values are obtained for different secondary anions with the proposed HSO_4^- ion-selective electrode, suggesting that these anions do not interfere in the normal working of the proposed electrode, even when present at high concentration levels of 1.0×10^{-2} M.

In addition, practical application of the proposed HSO_4^- ion-selective electrode was tested by employing it as an indicator electrode during the potentiometric titration of the hydrogen sulfate ion (20.0 mL, 1.0×10^{-2} M) against sodium hydroxide (1.0×10^{-2} M) solution. A sharp potential change near the end point indicated that the proposed electrode could be successfully used for monitoring potentiometric titrations (Fig. S14†).

In summary, we have designed and synthesized a new, coumarin-based, water-compatible, fluorescence 'turn-on' sensor (**1**) for HSO_4^- ions. Complexation studies by NMR, UV, and fluorescence spectroscopy were carried out towards different anions to demonstrate the sensor's excellent selectivity for the HSO_4^- ion over other anions tested. In the DFT calculations, application of the PET mechanism upon addition of HSO_4^- ions to **1** resulted in a pronounced 'Off–On' pattern in the fluorescence spectra. In addition, a remarkably selective potentiometric response was accomplished for the HSO_4^- ions over a variety of other anions using an ion-selective electrode based on **1**, incorporated into a polymeric (PVC) membrane. Hydrogen sulfate selectivity was due to the formation of a hydrogen bond between the phenolic –OH and the imine nitrogen atom in **1** and the HSO_4^- ions.

Table 3 Selectivity coefficients for the HSO_4^- ion-selective electrode

Secondary ions (B)	$\log K^{Pot}_{HSO_4^-,B}$	Secondary ions (B)	$\log K^{Pot}_{HSO_4^-,B}$
$CH_3CO_2^-$	−3.78	NO_2^-	−3.00
F^-	−2.95	CO_3^{2-}	−3.85
SCN^-	−3.20	Citrate	−4.44
NO_3^-	−4.00	$C_2O_4^{2-}$	−3.90
N_3^-	−3.05	$HCOO^-$	−2.90
CO_3^{2-}	−3.30	Br^-	−2.55
SO_4^{2-}	−4.75	I^-	−0.80
Cl^-	−1.00	$H_2PO_4^-$	−3.50

This work was supported by the CRI program, SRC (20090063001), and KRF-2008-313-C00501 of the National Research Foundation of Korea. JYL acknowledges the KOSEF (No. R11-2007-012-03002-0) and KRF (KRF-2008-313-C00388) grants by MEST.

Notes and references

‡ Single crystal data for **1**: $C_{17}H_{10}F_3NO_3$, M_w = 333.26, plate orange crystal, size: 0.30 × 0.30 × 0.30 mm^3, monoclinic, space group $P2_1/n$, a = 9.855(2) Å, b = 5.4280(11) Å, c = 26.716(5) Å, V = 1428.9(5) Å^3, T = 293(2) K, Z = 4, D = 1.549 Mg/m^3, ρ = 0.133 mm^{-1}, $F(000)$ = 680; 7321 reflections measured, of which 2796 were unique (R_{int} = 0.0552). 219 refined parameters, final R_1 = 0.0530 for reflections with $I > 2\sigma(I)$, wR_2 = 0.1541 (all data), GOF = 0.925. Final largest diffraction peak and hole: 0.192 and −0.236 e. Å^{-3}.

1 A. P. de Silva, H. Q. N. Gunaratne, T. Gunnlaugsson, A. J. M. Huxley, C. P. McCoy, J. T. Rademacher and T. E. Rice, *Chem. Rev.*, 1997, **97**, 1515; J. S. Kim and D. T. Quang, *Chem. Rev.*, 2007, **107**, 3780; H. N. Kim, M. H. Lee, H. J. Kim, J. S. Kim and J. Yoon, *Chem. Soc. Rev.*, 2008, **37**, 1465.

2 S. K. Kim, S. H. Lee, J. Y. Lee, R. A. Bartsch and J. S. Kim, *J. Am. Chem. Soc.*, 2004, **126**, 16499; S. K. Kim, J. H. Bok, R. A. Bartsch, J. Y. Lee and J. S. Kim, *Org. Lett.*, 2005, **7**, 4839; H.-F. Ji, G. M. Brown and R. Dabestani, *Chem. Commun.*, 1999, 609.

3 P. D. Beer, *Acc. Chem. Res.*, 1998, **31**, 71; M. J. Kim, R. Konduri, H. Ye, F. M. MacDonnell, F. Puntoriero, S. Serroni, S. Campagna, T. Holder, G. Kinsel and K. Rajeshwar, *Inorg. Chem.*, 2002, **41**, 2471.

4 Z. Xu, Y. Xiao, X. Qian, J. Cui and D. Cui, *Org. Lett.*, 2005, **7**, 889; J. B. Wang, X. F. Qian and J. N. Cui, *J. Org. Chem.*, 2006, **71**, 4308.

5 J.-S. Wu, J.-H. Zhou, P.-F. Wang, X.-H. Zhang and S.- K. Wu, *Org. Lett.*, 2005, **7**, 2133; B. Schazmann, N. Alhashimy and D. Diamond, *J. Am. Chem. Soc.*, 2006, **128**, 8607.

6 P. Ebbersen, *J. Immunol.*, 1972, **109**, 1296.

7 T. J. Grahame and R. B. Schlesinger, *Inhalation Toxicol.*, 2005, **17**, 15; P. I. Jalava, R. O. Salonen, A. S. Pennanen, M. S. Happo, P. Penttinen, A. I. Hälinen, M. Sillanpää, R. Hillamo and M.-R. Hirvone, *Toxicol. Appl. Pharmacol.*, 2008, **229**, 146.

8 J. L. Sessler, E. Katayev, G. D. Pantos and Y. A. Ustynyuk, *Chem. Commun.*, 2004, 1276; R. Shen, X. Pan, H. Wang, L. Yao, J. Wu and N. Tang, *Dalton Trans.*, 2008, 3574; N. Singh, N. Kaur, J. Dunn, R. Behan, R. C. Mulrooney and J. F. Callan, *Eur. Polym. J.*, 2009, **45**, 272.

9 See Electronic Supplementary Information (ESI).

10 Association constants were calculated using the computer program ENZFITTER, available from Elsevier-BIOSOFT, 68 Hills Road, Cambridge, UK CB2 1LA; K. A. Connors, *Binding Constants*, Wiley, New York, 1987.

11 M. J. Frisch, *et al.*, *GAUSSIAN 03 (Revision D.02)*, Gaussian, Inc., Pittsburgh, PA, 2006.

12 M. Chanon, M. D. Hawley and M. A. Fox, in *Photoinduced Electron Transfer*, ed. M. A. Fox and M. Chanon, Elsevier, Amsterdom, 1988, part A, p. 1.

13 R. K. Mahajan, I. Kaur, R. Kaur, A. Onimaru, S. Shinoda and H. Tsukube, *Anal. Chem.*, 2004, **76**, 7354.

